Effect of unequal vaccination coverage and migration on long-term pathogen evolution in a metapopulation

Alicia Walter[1], Sylvain Gandon[2] , Sébastien Lion[3]

December 16, 2022

CEFE, CNRS, Univ Montpellier, EPHE, IRD, Montpellier, France

[1] E-mail: alicia.walter@cefe.cnrs.fr. ORCID: 0000-0002-7334-0247

[2] E-mail: sylvain.gandon@cefe.cnrs.fr. ORCID: 0000-0003-2624-7856

[3] E-mail: sebastien.lion@cefe.cnrs.fr. ORCID: 0000-0002-4081-0038

Key-words: virulence evolution, vaccination, metapopulation, polymorphism, spatial heterogeneity

Abstract

Worldwide inequalities in vaccine availability are expected to affect the spread and spatial distribution of infectious diseases. It is unclear, however, how spatial variation in vaccination coverage can affect the long-term evolution of pathogens. Here we use an analytical model and numerical simulations to analyse the influence of different imperfect vaccines on the evolution of pathogen virulence in a two-population model where vaccination coverage varies between populations. We focus on four vaccines, with different modes of action on the life-cycle of a pathogen infecting two host populations coupled by migration. We show that, for vaccines that reduce infection risk or transmissibility, spatial heterogeneity has little effect on pathogen prevalence and host mortality, and no effect on the evolution of pathogen virulence. In contrast, vaccines that reduce pathogen virulence can select for more virulent pathogens and may lead to the coexistence of different pathogen strains, depending on the degree of spatial heterogeneity in the metapopulation. This heterogeneity is driven by two parameters: pathogen migration and the difference in the vaccination rate between the two populations. We show that vaccines that only reduce pathogen virulence select mainly for a single pathogen strategy in the long term while vaccines that reduce both transmission and virulence can favor the coexistence of two pathogen genotypes.We discuss the implications and potential extensions of our analysis.

1 Introduction

Vaccines that reduce pathogen spread or harmfulness are a key tool for the management of infectious diseases in human and animal populations. At the same time, vaccination, like other public health measures, may affect the selective pressures on pathogens and potentially lead to the evolution of higher or lower virulence and transmission (Read et al., 2015; Gandon and Day, 2008). Hence, a major challenge when designing public health measures, notably vaccination campaigns, is to balance the often urgent need to manage epidemic and endemic infectious diseases with potential long-term evolutionary side-effects

(Dieckmann et al., 2005; Day et al., 2020). Theoretical studies have shown that, in the long run, imperfect vaccines may select for higher or lower pathogen virulence depending on the mode of action of the vaccine and on the characteristics of the environment experienced by the pathogen (notably vaccination coverage, spatial structure and temporal heterogeneity) (Gandon et al., 2001, 2003; Zurita-Gutiérrez and Lion, 2015; Walter and Lion, 2021).

However, human and animal populations are often characterised by heterogeneity in vaccination coverage and complex patterns of dispersal between local populations. For instance, in human populations, different regions, even geographically close, may have very different coverage of vaccination, as exemplified by regional differences in vaccination against measles in the Netherlands (Knol et al., 2013) or the worldwide inequality of access to COVID-19 vaccines (Mathieu et al., 2021; Rydland et al., 2022). Furthermore, the globalization of travel and trade tends to increase the connections between local populations and to facilitate the dispersal of hosts and pathogens, with potentially worrying consequences for pathogen spread and evolution (Memish et al., 2015; Boots and Sasaki, 1999). Hence, host populations are best viewed as metapopulations of local patches with different epidemiological characteristics, coupled by host or pathogen migration. It is not clear how the interplay between migration and spatial heterogeneity in vaccine coverage will affect the epidemiology and evolution of pathogens.

As a first step towards answering this question, we analyse a theoretical model to understand the combined effects of migration and vaccine distribution on the long-term evolution of pathogen virulence in a metapopulation. Our study is motivated by local adaptation models that have shown that a metapopulation with migration between subpopulations can select for generalist or specialist strategies depending on migration and the degree of similarity between the populations (Meszéna et al., 1997; Day, 2000; Ronce and Kirkpatrick, 2001; Débarre et al., 2013; Mirrahimi and Gandon, 2020). Here, we ask how these factors may affect the evolution of pathogen polymorphism and what are the implications of such polymorphism for the epidemiological and evolutionary management of diseases.

We study a metapopulation of two subpopulations connected by migration. Each population contains naive and vaccinated hosts in different frequencies. Following Gandon et al. (2001), we assume the vaccine is imperfect, and can have different modes of action on the pathogen's life cycle. Moreover, we consider a heterogeneous vaccine distribution across the two populations, and explore the epidemiological and evolutionary consequences of different vaccine distributions, ranging from homogeneous (i.e. equal distribution between the two subpopulations) to fully heterogeneous (i.e. one population is completely vaccinated and the other completely naive) distributions. We investigate, both analytically and numerically, the long-term effects of spatial heterogeneity on the evolution of pathogen virulence, either for vaccines with a single mode of action, or for vaccines combining different modes of action on the pathogen's lifecycle. We present and discuss the epidemiological and evolutionary consequences of these different scenarios, as well as the broader implications of our study for infectious disease management.

2 Epidemiological model

We consider a metapopulation composed of two subpopulations A and B, that are coupled by parasite migration (life cycle depicted in **figure 1**, see table 1 for notations). In each subpopulation, the host-pathogen interaction is described by a susceptible-infected epidemiological model. Susceptible hosts are produced in each subpopulation at rate b, and vaccinated with a habitat-specific probability. In subpopulation A, a proportion ν_A of new hosts receive the vaccine and enter the vaccinated class S_A^T, while a proportion $1-\nu_A$ enter the unvaccinated class S_A^N. Likewise, in subpopulation B, a proportion ν_B of new hosts enter the S_B^T class, and a proportion $1-\nu_B$ enter the S_B^N class. (Note that this can

be interpreted as a model of vaccination at birth, but we show in *Supplementary Information S.1* that an alternative model where adults are vaccinated leads to qualitatively identical results.). All hosts die at a natural rate d. The metapopulation is infected by a pathogen that can migrate between the two subpopulations at rate m, which varies between 0 and 0.5. For $m = 0$, there is only local transmission of pathogens and susceptible hosts of population A (respectively B) are only infected by infected hosts from population A (respectively B). For $m = 0.5$, susceptible hosts can be equally infected by hosts from population A or B. We consider that scenarios where m is greater than 0.5, meaning that susceptible hosts would be more infected by hosts from the other subpopulation, would be unrealistic (Park et al., 2015). Infected hosts transmit the pathogen at rate β_A or β_B and have an additional disease induced mortality rate which differs for naive (α_A^N and α_B^N) and vaccinated hosts (α_A^T and α_B^T). These assumptions lead to the the following ODE system for the subpopulation j :

$$\begin{aligned}
\frac{\mathrm{d}S_j^N}{\mathrm{d}t} &= b(1-\nu_j) - S_j^N(d + H_j^N)\,, \\
\frac{\mathrm{d}S_j^T}{\mathrm{d}t} &= b\nu_j - S_j^T(d + H_j^T)\,, \\
\frac{\mathrm{d}I_j^N}{\mathrm{d}t} &= S_j^N H_j^N - (d + \alpha_j^N) I_j^N\,, \\
\frac{\mathrm{d}I_j^T}{\mathrm{d}t} &= S_j^T H_j^T - (d + \alpha_j^T) I_j^T\,,
\end{aligned} \tag{1}$$

where j represents the population A or B, and H_j (resp. H_j^T) is the force of infection experienced by a naive (resp. vaccinated) susceptible host in population j. This force of infection depends on pathogen migration and is a weighted average of the contributions of infected hosts in populations A and B, so that $H_j = (1-m)h_j + mh_{\bar{j}}$, where we use the notation $\bar{j}$ to refer to the non-focal population j (i.e., $\bar{j} = B$ if $j = A$), and h_j is the force of infection on hosts in population j:

$$h_j = \beta_j^N I_j^N + \beta_j^T I_j^T \tag{2}$$

where β_j^N (resp. β_j^T) is the pathogen's transmission rate in class N (resp. T) in subpopulation j. Analogous expressions can be derived for population B, leading to a 8-equation ODE system which is given in *Supplementary Information S.2*.

Following Gandon et al. (2001, 2003), we consider four imperfect vaccines with different modes of actions on the pathogen's lifecycle. We assume that the vaccine can either (1) reduce the susceptibility of hosts (anti-infection vaccine, noted r_1), (2) reduce the within-host growth rate of pathogens (anti-growth vaccine, noted r_2), (3) reduce pathogen transmission (anti-transmission vaccine, noted r_3) and (4) reduce disease-induced mortality in infected hosts (anti-virulence vaccine, noted r_4). Biological examples of each type of vaccine are presented in Walter and Lion (2021).

With these assumptions, the typical epidemiological behaviour of our model is either pathogen extinction or convergence to an endemic state where the densities of all classes of susceptible and infected hosts settle on equilibrium values. In the following we consider how the migration rate m, and the probabilities of vaccination ν_A and ν_B affect these endemic equilibria and the long-term evolutionary outcome of the pathogen population. In the next section we use adaptive dynamics to study long-term evolution of the pathogen population in a two-patch metapopulation with uneven vaccination coverage, before applying the results to specific epidemiological scenarios.

(a) Local dynamics in population j

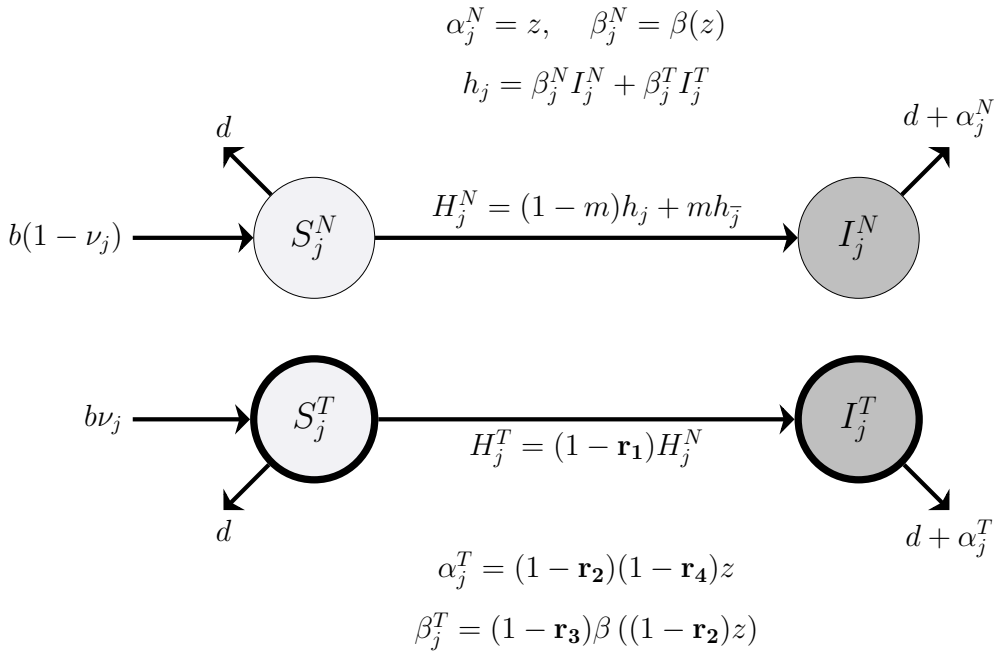

(b) Global dynamics at the metapopulation level

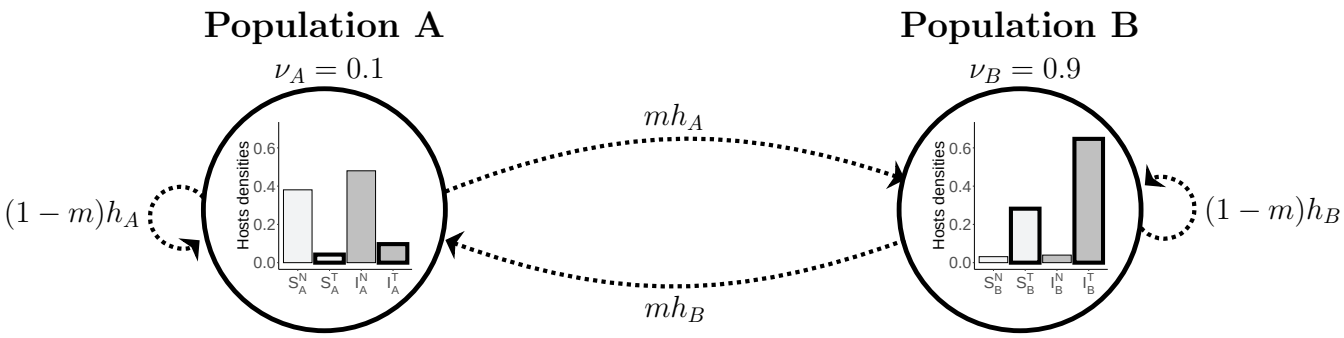

Figure 1: (a) Life cycle of the host-pathogen interaction in the population j, showing transition rates between classes. Susceptible hosts are represented in light grey and infected hosts in dark grey, vaccinated hosts are in thick circle and naive hosts in thin. The expressions are explained in the main text. (b) Transition rates in the metapopulation showing how pathogens migration m affects the forces of infection. Barplots of hosts densities are shown as examples of populations structure at equilibrium with an anti-virulence vaccine, where $\nu_A = 0.1$, $\nu_B = 0.9$, $r_4 = 0.8$, $b = 2$ and $d = 1$.

Table 1: Table of parameters and variables.

Parameter	Definition
	Life history traits
α_j^k	disease-induced mortality caused by the pathogen strain in population j and class k
β_j^k	transmission of the disease of the pathogen strain in population j and class k
h_j	production of propagules by hosts in population j
H_j	force of infection caused by hosts in population j
	Reproductive values
c_j	class reproductive value in population j
	Ecology
b	influx of susceptible hosts
d	natural death rate
m	parasite migration rate
	Vaccines
ν_j	probability of vaccinating new hosts in population j
δ	$\nu_B - \nu_A$
r_1	efficacy of anti-infection vaccine
r_2	efficacy of anti-growth vaccine
r_3	efficacy of anti-transmission vaccine
r_4	efficacy of anti-virulence vaccine

k stands for naive (N) or vaccinated (T) hosts
j stands for population A or B

3 Evolutionary dynamics

Assuming that the metapopulation infected by a resident strain of the pathogen has reached an epidemiological equilibrium, we consider a scenario where a mutant strain of the pathogen strain appears with different life-history traits, and investigate the invasion success of this mutant using the adaptive dynamics framework (Geritz et al., 1998; Dieckmann et al., 2005).

3.1 Mutant invasion fitness

Consider that the resident pathogen has trait z and that a mutant strain appears in the metapopulation with a different trait value, noted z'. We assume that both transmission and virulence are functions of the trait z (we will provide explicit examples for these functions in section 3.4) and, consequently, the mutation leads to different life-history traits for the mutant pathogen, denoted by a prime (e.g. $\alpha_A'^N$ is the virulence caused by the mutant pathogen in naive infected hosts in population A). The mutant can either die out or invade and replace the resident strain. Mutant success depends on its invasion fitness, $R(z, z')$, that represents the number of surviving mutant offspring per mutant parent when the mutant allele is rare (Hurford et al., 2009; Otto and Day, 2011). In our model this takes the form (*Supplementary Information S.3*) :

$$R(z, z') = \frac{1}{2}\left((1-m)(R'_A + R'_B) + \sqrt{4(2m-1)R'_A R'_B + (1-m)^2(R'_A + R'_B)^2}\right) , \tag{3}$$

with

$$R'_j = R'^N_j \hat{S}^N_j + \sigma R'^T_j \hat{S}^T_j \tag{4}$$

the mutant invasion fitness in the subpopulation j (A or B), where

$$R'^N_j = \frac{\beta'^N_j}{(d + \alpha'^N_j)} \quad \text{and} \quad R'^T_j = \frac{\beta'^T_j}{(d + \alpha'^T_j)} \tag{5}$$

are respectively the mutant reproduction numbers in naive or vaccinated hosts in population j. Note that the invasion fitness of the mutant, $R(z, z')$, depends both on the resident trait through susceptible densities at equilibrium $\hat{S}^N_j$ and $\hat{S}^T_j$ (included in R'_A and R'_B), and on the mutant trait through the transmissibility (β'^N_j and β'^T_j) and virulence (α'^N_j and α'^T_j) traits, which are included in R'^N_j and R'^T_j. The mutant invades if $R(z, z') > 1$, and dies out if $R(z, z') \leq 1$

3.2 Selection gradient

In order to gain analytical insight on the long-term evolution of the trait of interest, z which governs the virulence and the transmission of the pathogen, we calculate the selection gradient, $\mathcal{S}$. This amounts to calculating the partial derivative of the mutants invasion fitness $R(z, z')$ with respect to z' evaluated at $z = z'$. The zeros of the selection gradient correspond to the evolutionary singularities, noted z^*. In our model, it can be expressed as (*Supplementary Information S.3*) :

$$\mathcal{S} = c_A \frac{\partial R'_A}{R_A} + c_B \frac{\partial R'_B}{R_B} \tag{6}$$

where $\partial R'_j$ are the derivative of the mutant reproduction number with respect to z' evaluated at $z = z'$, in the supopulation j (see *Supplementary Information S.4* for a full expression), and

$$c_A = R_A \frac{R_B(2m-1) + (1-m)}{2 + (m-1)(R_A + R_B)} \qquad \text{and} \qquad c_B = R_B \frac{R_A(2m-1) + (1-m)}{2 + (m-1)(R_A + R_B)} \tag{7}$$

are the class reproductive values of pathogens in populations A and B respectively. The class reproductive values sum to 1 (e.g. $c_A + c_B = 1$, see *Supplementary Information S.3*) and can therefore be interpreted as measures of host quality for the pathogen which weight the effects of selection in the two populations (Rousset, 1999; Gandon, 2004; Lion, 2018; Walter and Lion, 2021; Lion and Gandon, 2021). When the two populations are isolated ($m = 0$), there are two distinct singularities for each subpopulation, $z^\star_A$ and $z^\star_B$, which corresponds to the zeros of $\partial R'_A$ and $\partial R'_B$ respectively. In the extreme case where a subpopulation (say, A) represents a habitat of very poor quality for pathogens (e.g. c_A tends towards 0), then, at the metapopulation level, the singularity $z^\star$ will tend towards the singularity of the good habitat, $z^\star_B$. On the other hand, when the two populations have similar qualities ($c_A = c_B = 1/2$), the singularity at the metapopulation level will be intermediate between $z^\star_A$ and $z^\star_B$.

3.3 Second-order derivative

After convergence by successive mutations towards an evolutionary singularity, two different outcomes are possible. If the singularity cannot be invaded by nearby mutants, it corresponds to an evolutionarily stable strategy (ESS). If nearby mutants can invade, the singularity is called a branching point (BP), and the population can split into two coexisting morphs. The stability of the singularity can be investigated by calculating the second-order derivative of the invasion fitness, $\mathcal{D}$, near the singularity $z^\star$. If $\mathcal{D} < 0$ the

evolutionary singularity is stable. If $\mathcal{D} > 0$, the singularity is unstable. In our model, $\mathcal{D}$ takes the form

$$\mathcal{D} = c_A \frac{\partial^2 R'_A}{R_A} + c_B \frac{\partial^2 R'_B}{R_B} + \kappa\,, \tag{8}$$

where $\partial^2 R'_j$ is the second order derivative of the mutant reproduction number in population j with respect to z' evaluated at $z = z'$ (see *Supplementary Information S.4* for a full expression), and

$$\kappa = 2(c_A c_B)^{3/2}\sqrt{R_A R_B}\left(\frac{\partial R'_A}{R_A} - \frac{\partial R'_B}{R_B}\right)^2 \frac{1-2m}{m}. \tag{9}$$

It is useful to interpret equations (8) by using the analogy of the fitness landscape. The first two terms on the right-hand side of equation (8) are a weighted average of the local curvature of the fitness landscapes in populations A and B, while κ in equation (9) depends on the squared difference of the slopes of the fitness landscapes, locally near the singularity. Note that κ is always positive, and therefore acts as a destabilising force. Hence, for $z^\star$ to be a local fitness maximum (and therefore an ESS), it is not sufficient that it is a fitness maximum in both populations, as disruptive selection emerges if the direction of selection is sufficiently different in the two populations (leading to sufficiently positive values of κ).

In the limiting case where $\kappa = 0$, however, the sign of $\mathcal{D}$ is only determined by the weighted average of the curvatures. With a concave saturating transmission-virulence trade-off, both $\partial^2 R'_A$ and $\partial^2 R'_B$ are negative, and therefore z^* is always an ESS. From equation (9), we see that this can occur when (1) the class reproductive value of the pathogen is zero in one of the populations (e.g. $c_A c_B = 0$); (2) the direction of selection is the same in both habitats (e.g. $\partial R'_A = \partial R'_B$); and (3) the metapopulation is well-mixed ($m = 1/2$).

It is also interesting to examine the limit case where the migration rate is small because we can approximate κ as follows:

$$\kappa \sim \left(\partial R'_A - \partial R'_B\right)^2 \frac{1-2m}{4m}\,, \tag{10}$$

Thus, when $m \to 0$, κ diverges towards infinity. Hence, the singularity will tend to be unstable at low migration rates, unless the two populations resemble a single population (either because direction selection is equal in both ($\partial R'_A = \partial R'_B$) or because one of the populations does not contribute to selection ($c_A = 0$ or $c_B = 0$).

Away from these limiting cases the singular strategies will be stable if $\kappa < c_A \partial^2 R'_A + c_B \partial^2 R'_B$ (i.e., $\mathcal{D} < 0$ and unstable otherwise. In the following we explore the balance between the forces acting on the stability of the singular strategies with numerical examples.

3.4 Numerical examples

In the following we first focus on a scenario where the host is vaccinated with a single vaccine at a time (either anti-infection, anti-transmission, anti-growth or anti-virulence), and we vary the efficacy of the vaccine between 0 (ineffective vaccine) and 1 (perfect vaccine). In line with previous theoretical studies on virulence evolution (Alizon et al., 2009), we assume a positive correlation between transmission and virulence, captured by an increasing and saturating transmission-virulence trade-off function. More specifically we use $\beta[z] = 5z/(1+z)$ in all our simulations.

We assume that the average probability of vaccination at birth is $\nu = (\nu_A + \nu_B)/2 = 0.5$. We aim to compare a homogeneous distribution of vaccines among the two subpopulations ($\nu_A = \nu_B$), to a heterogeneous distribution of vaccines ($\nu_A \neq \nu_B$). We assume that the vaccination coverage is always

higher in population B than in population A ($\nu_B \geq \nu_A$, with $\nu_A \in [0, 0.5]$ and $\nu_B \in [0.5, 1]$). To quantify the variation in vaccination coverage we introduce the parameter $\delta = \nu_B - \nu_A$ that varies between 0 (homogeneous distribution, $\nu_A = \nu_B$) and 1 (fully heterogeneous distribution, $\nu_B = 1$, $\nu_A = 0$). Moreover, we focus on highly effective vaccines ($r_j = 0.9$, with $j \in \{1, 2, 3, 4\}$, i.e. the vaccine is 90% effective) but other parameter values are explored in the Supplementary Information.

Anti-infection and anti-transmission vaccines For anti-infection (r_1) or anti-transmission (r_3) vaccines, we show that spatial structure does not affect pathogen evolution (*Supplementary Information S.5*). The ES virulence depends neither on the migration rate m nor on the variation in vaccination coverage δ. This is consistent with previous results obtained in well-mixed single-population models (Gandon et al., 2001; Zurita-Gutiérrez and Lion, 2015; Walter and Lion, 2021). In the following, we therefore focus on anti-growth (r_2) and anti-virulence (r_4) vaccines.

Anti-growth and anti-virulence vaccines Non-spatial models have shown that anti-growth (r_2) and anti-virulence (r_4) vaccines can select for increased virulence (Gandon et al., 2001, 2003; Read et al., 2015; Walter and Lion, 2021). Our results show that, in line with these earlier results, both r_2 and r_4 vaccines select for higher virulence. This effect is also modulated by the migration rate m and the heterogeneity in vaccination coverage δ, which can lead to different type of singularities in the long-term: (i) a single ESS, (ii) a branching point or (iii) a bistability with two ESS that surround a repellor (a representation of the three possible outcomes is represented in *Supplementary Information S.3*).

Figure 2 illustrates the effect of the migration m, on the singularities, for a fixed value of the vaccination heterogeneity δ. With high migration (i.e. $m = 0.5$) we observe a single evolutionary stable virulence. As the migration decreases and the two populations become disconnected, the singularity turns into a branching point, leading to the coexistence of two pathogens strains. As migration further decreases, the model exhibits evolutionary bistability, with two locally stable ESSs separated by a repellor. Our AD analysis predicts that one of the two ESSs will be reached depending on the initial trait value. However, in numerical simulations where the AD assumptions are relaxed, we always observe a dimorphic trait distribution. This is because there is always a globally stable dimorphic attractor (the dots in **figure 2**) in addition to the locally stable monomorphic singularities (*Supplementary Information S.3*). A similar result was obtained by Débarre et al. (2013); Mirrahimi and Gandon (2020) in a local adaptation model.

In figure 3, we explore the interaction between the effects of the heterogeneity in vaccination coverage δ and migration on pathogen evolution. In each of these figures, the bottom right corner corresponds to the most heterogeneous metapopulation (low migration and maximal difference in vaccination coverage). In contrast, the upper-left corner represents a completely homogeneous metapopulation ($\delta = 0$ and $m = 0.5$), and corresponds to the results of Gandon et al. (2001) (without superinfection) or Walter and Lion (2021) (without temporal fluctuations). As expected, when δ increases (i.e. selection between populations becomes more divergent), polymorphism emerges more readily.

Both **figures 2** and **3** show that anti-growth vaccines (r_2) promote the coexistence between a low and a high virulence pathogen when migration is low. In contrast, anti-virulence vaccines ($r4$) is less prone to the emergence of polymorphism.

In **figure 4** we explore the effects of a a vaccine that combines multiple components on the evolution of the pathogen. In particular, **figure 4a** shows that the combination of r_2 and r_4 effects can further expand the parameter space where polymorphism is expected to emerge and be stably maintained in the long-term. In particular, note that polymorphism can become stable even with full migration (i.e., $m = 0.5$). However, this effect is complex and non-monotonous (e.g., the effect of an increase in r_4 on the

maintenance of polylmorphism). In **figure 4b** we also explore the effect of a vaccine with a combination of r_2 and r_1 effects. **Figure 4b** shows that even if r_1 is expected to have no effect on pathogen evolution, we see a major interaction with the effect of r_2 since r_1 reduces the possibility of bistability and branching. A similar effect is observed in a combination between r_2 and r_3 (see *Supplementary Information S.6*).

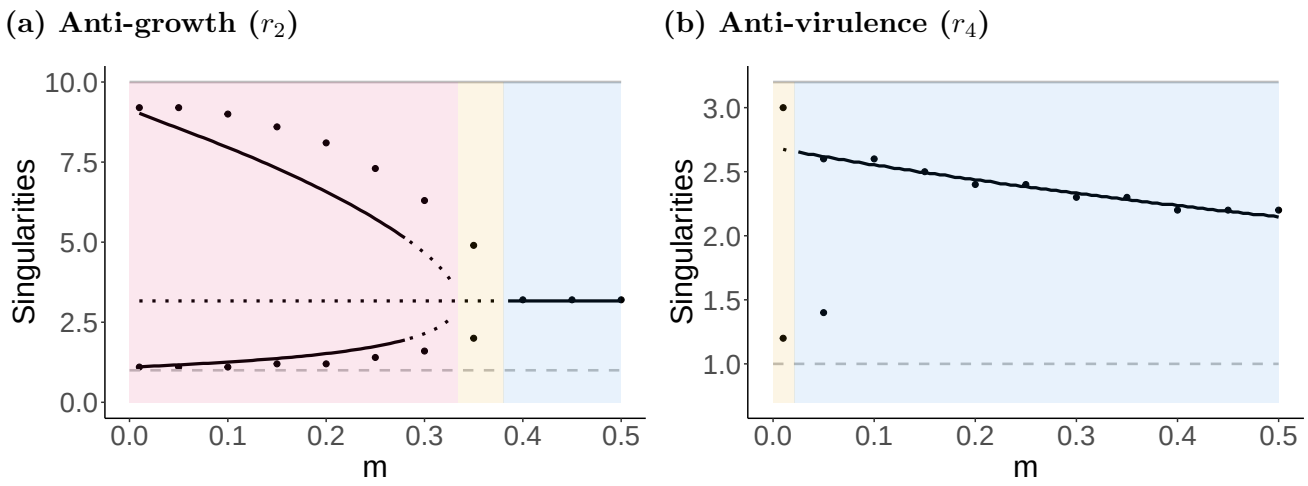

Figure 2: The singularities (in black) are calculated using adaptive dynamics, ESS's are in plain lines and branching points or repellors in dotted lines. The dashed grey lines represent the ESS without vaccination and the plain grey lines represent the ESS with a full vaccination.The ESS area is represented in light blue, branching point in light orange and bistability in light pink. The black dots represent the singularity with respect to m, calculated using the framework explained in *Supplementary Information S.7* (the simulation in ran 10 000 time steps, $\mu = 0.001$, $V_m = 0.01$) and , for (a) $r_2 = 0.9$ and (b) $r_4 = 0.9$. Here $\delta = 0.75$ and all the other parameters as in **figure 1**.

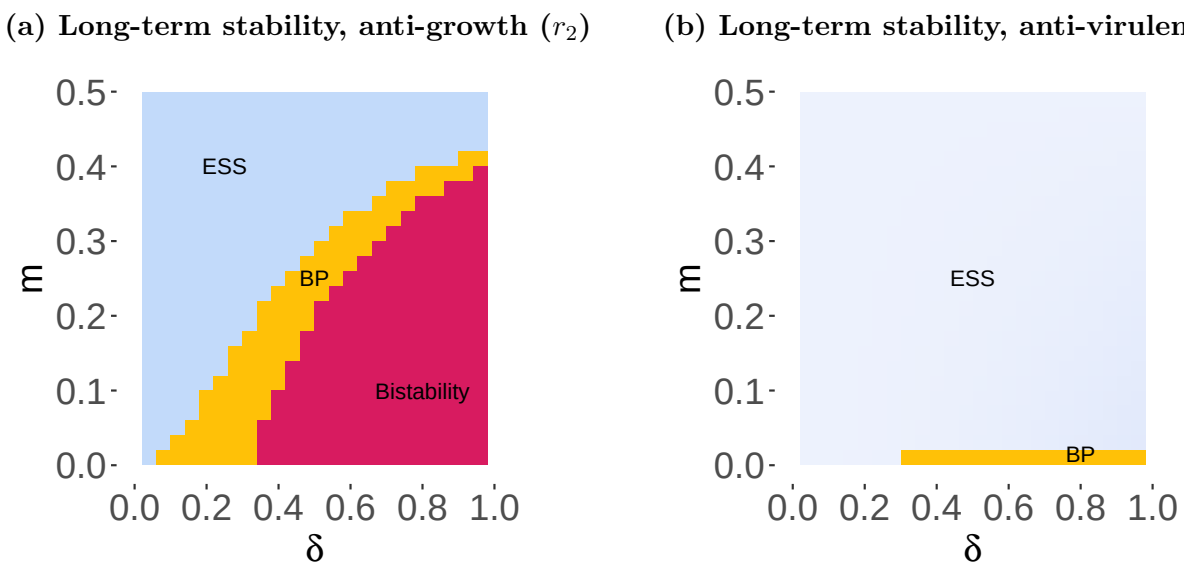

Figure 3: Long term evolutionary state calculated using adaptive dynamics, for (a) anti-growth and (b) anti-virulence vaccines. Evolutionary stable virulence (ESS) are represented in blue, following the gradient shown in **figure 4**, branching point (BP) in orange and bistability in pink, according to m and δ. Here $r_j = 0.9$ and the other parameters are as in **figure 1**.

(a) Anti-growth (r_2) combined with anti-virulence (r_4) vaccine

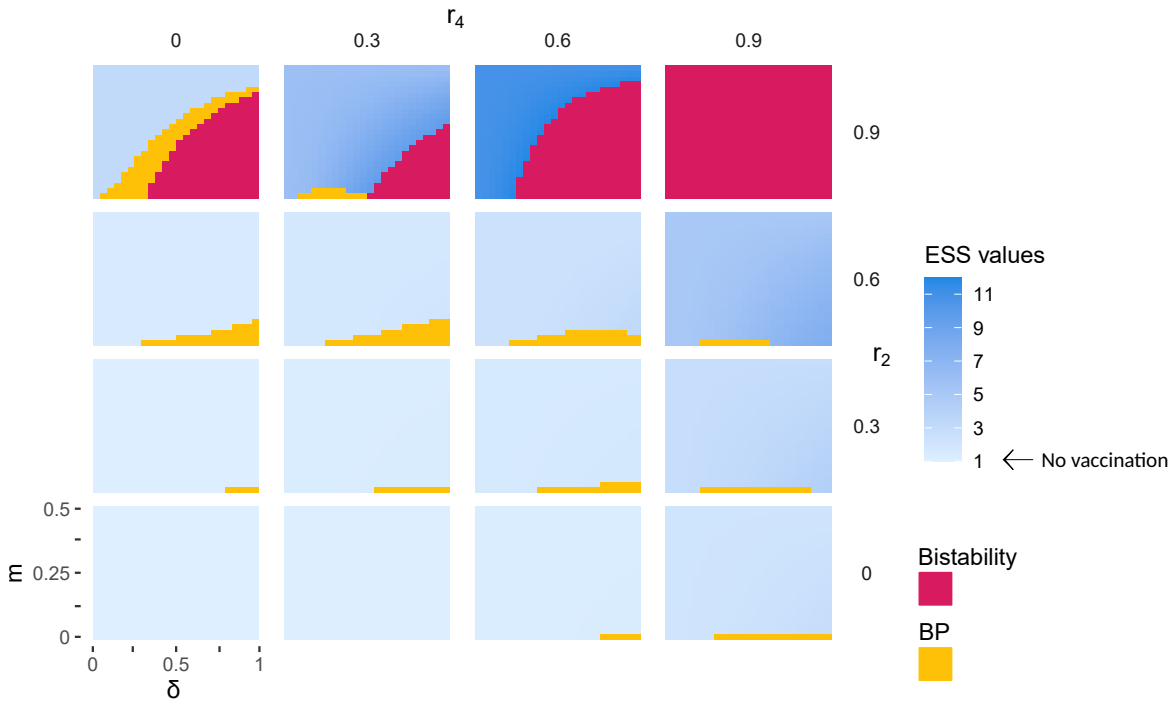

(b) Anti-growth (r_2) combined with anti-infection (r_1) vaccine

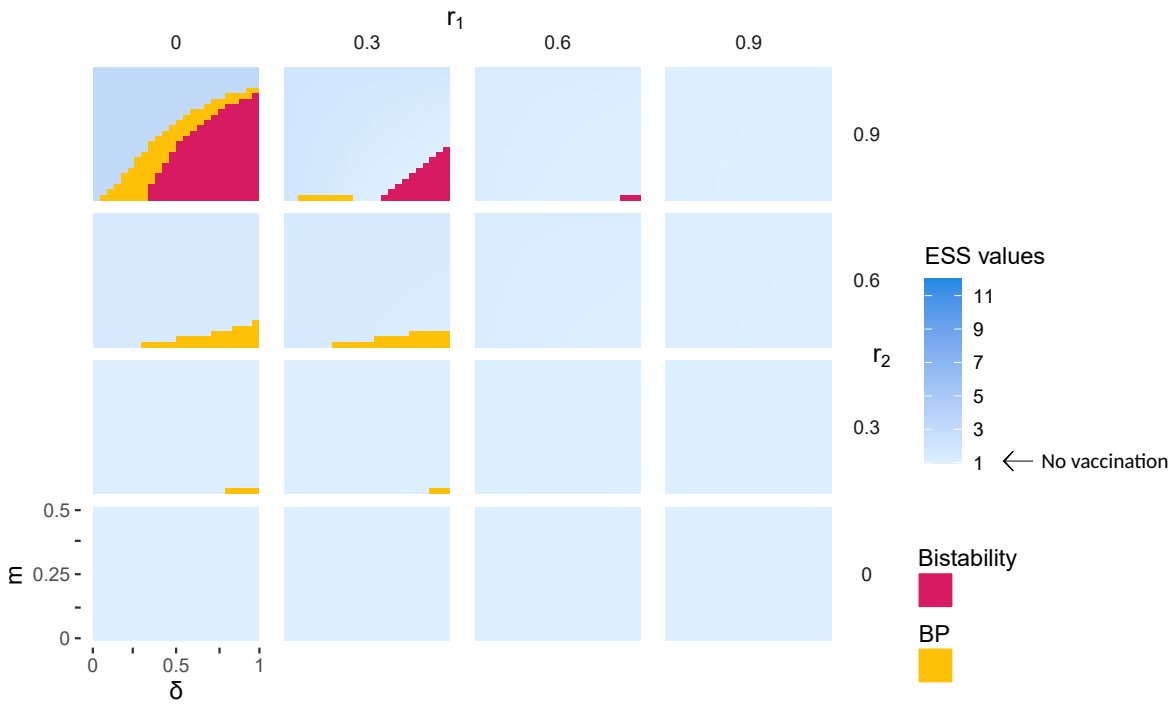

Figure 4: Long term evolutionary state calculated using adaptive dynamics, for anti-growth vaccine combined with anti-virulence, according to m and δ. Branching point (BP) are represented in yellow, bistability in pink, and ESS values in a gradient of blue. Other parameters as in **figure 1**.

4 Discussion

Here we study the long-term evolution of pathogen life-history traits in a metapopulation, in response to the selective pressures caused by imperfect vaccines with different modes of action. Our first result is that anti-infection and anti-transmission vaccines have no effect on the long-term evolution of pathogen virulence. This is fully consistent with the predictions of earlier non-spatial models (Gandon et al.,

2001, 2003; Walter and Lion, 2021). However, for anti-growth and anti-virulence vaccines, we show that the long-term evolutionary outcomes crucially depend on the degree of spatial heterogeneity of the metapopulation, which we quantify using two parameters: the migration rate m and the asymmetry in vaccine coverage δ. For high migration ($m = 0.5$) and low asymmetry ($\delta = 0$), the metapopulation behaves like a single homogeneous population, as in previous non-spatial models (Gandon et al., 2001, 2003; Walter and Lion, 2021). However, when migration is low and assymmetry is high, pathogen polymorphism becomes possible, leading to coexistence between two specialist strains, one that is adapted to the less vaccinated population, and the other that is adapted to the population with higher coverage. In other words, as in classical metapopulation models (Meszéna et al., 1997; Day, 2000; Ronce and Kirkpatrick, 2001; Débarre et al., 2013; Mirrahimi and Gandon, 2020), heterogeneity in selection (as measured by the asymmetry δ) and low migration favours the coexistence between genotypes locally adapted to each habitat. When the degree of heterogeneity of the metapopulation is below a threshold, our model predicts a single generalist ES strategy.

In contrast to classical local adaptation models which tend to assume Gaussian fitness functions maximized at fixed and externally determined optima, the effects we observe in our vaccination model are all mediated by epidemiological feedbacks, through the densities of vaccinated and unvaccinated infected hosts in each subpopulation. Interestingly, these epidemiological feedbacks act differently for anti-growth (r_2) and anti-virulence (r_4) vaccines: increasing the degree of heterogeneity in the metapopulation selects for more diversification with anti-growth vaccines, while polymorphism is only observed for maximal heterogeneity with anti-virulence vaccines. However, increasing heterogeneity has a negligible effect on ES virulence for r_2 vaccines, whereas it selects for increased virulence with r_4 vaccines. This occurs because r_4 vaccines increases the duration of infection and therefore leads to much higher disease prevalence in the highly vaccinated population, which causes asymmetric migration between the two host populations. Pathogen migration from the vaccinated population has two consequences. First, it prevents adaptation to non-vaccinated hosts and selects for high ES virulence. Second, asymmetric migration prevents the coexistence between two specialist genotypes because local selection to the unvaccinated population is swamped by migration from the vaccinated population. This source-sink interpretation is similar to the findings of earlier analyses of adaptation in two-population models (Meszéna et al., 1997; Day, 2000; Ronce and Kirkpatrick, 2001; Débarre et al., 2013; Mirrahimi and Gandon, 2020). This source-sink dynamics is very different with the anti-growth (r_2) vaccine because pathogen prevalence drops in the vaccinated population.

Although the results in the main text assume a high vaccine efficacy (90%) and that the mean vaccination coverage at birth is 1/2 (and thus, $(\nu_B + \nu_A)/2 = 1/2$), we have relaxed these assumptions in *Supplementary Information S.8*, where we generalise our results to all the possible combinations of vaccine coverage and efficacy. We show that an increase in pathogen migration, a decrease in vaccination asymmetry and a decrease in vaccine efficacy makes polymorphism less likely. This is consistent with our general message that, as the metapopulation becomes increasingly homogeneous, the potential for diversification weakens. In *Supplementary Information S.1*, we also show that a model where adults (and not newborns) are vaccinated yields qualitatively similar predictions.

From an applied point of view, the consequences of the evolution of pathogen polymorphism on long-term infectious disease management is unclear. On the one hand, our model does not predict that polymorphism affects the cumulative number of deaths (see *Supplementary Information S.9*), although this specific prediction is probably sensitive to epidemiological assumptions. On the other hand, the circulation of two variants instead of one is a major challenge for the design of effective control strategies. For instance, this may require the development of vaccines targeting all strains, or specifically the

most virulent variants as in the vaccination against *Streptococcus pneumoniae* (Masomian et al., 2020; Musher et al., 2022) or against human papillomavirus (Schiller and Lowy, 2012; Koutsky and Harper, 2006) Further studies are thus required to investigate how strain coexistence, which is expected to be a qualitatively robust outcome of pathogen evolution in populations with a high degree of spatial heterogeneity, needs to be taken into account in public health strategies.

It is interesting to compare the predictions of our two-patch model to previous analyses of the impact of spatial structure on the evolution of pathogen virulence. Using a lattice model, Zurita-Gutiérrez and Lion (2015) have shown that, for all types of vaccines, lower pathogen dispersal tends to select for lower ES virulence, except for high-efficacy anti-growth vaccines. In addition, they do not observe polymorphism. Although this prediction is consistent with the result that selection should favour more "prudent" pathogen strains in spatially structured populations (Haraguchi and Sasaki, 2000; Van Baalen, 2002; Lion and Baalen, 2008), it could appear at odds with our result that pathogen migration either has no or little effect on the ES virulence (for r_1, r_2 and r_3 vaccines) or leads to increased ES virulence (for r_4 vaccines) or to polymorphism. However, it is important to note that, although the model of Zurita-Gutiérrez and Lion (2015) does incorporate spatial structure by allowing a mixture of global and local transmission, it does not allow for heterogeneity in vaccination coverage as all new hosts have the same probability of being vaccinated, irrespective of their location. Furthermore, the effects observed in Zurita-Gutiérrez and Lion (2015) are mostly driven by kin competition for susceptible hosts. In our model, local populations are well-mixed and there is no kin selection.

There are several interesting potential extensions of this work. First, although we have framed our results in the context of vaccination against a pathogen infecting a single species of hosts, our analytical results are more general because they allow the pathogen's life-history traits to depend on different types of host (N and T in the present model). This implies that the same analytical expressions capture the direction of selection and the condition of evolutionarily stability for a pathogen infecting two host species (Gandon, 2004). Moreover, the focus on vaccines is by no means exclusive, as the four modes of action we distinguish can also be used to describe the action of other forms of heterogeneity, such as genetic resistance in the host or other treaments. Second, a limitation of our study is that it relies on a separation of time scales assumption to make prediction on the long-term evolutionary outcome. However, for many practical purposes, what matters most is the joint dynamics of strain diversity and epidemiological dynamics over shorter time scales (Gandon and Lion, 2022). Hence, it would be interesting to extend this model to take into account both spatial heterogeneity and epidemic dynamics on the transient spread of new pathogen variants. Third, our adaptive dynamics framework is not well suited to capture the inherently stochastic nature of the spread of new mutations (Restif and Grenfell, 2006, 2007; Day et al., 2022; Gandon et al., 2022). In a similar two-patch stochastic model, Gerrish et al. (2021) have shown that heterogeneity in vaccine distribution promotes the emergence of vaccine escape mutants. It would be interesting to explore how demographic stochasticity could alter the emergence and the spread of new pathogen variants.

At a conceptual level, there is a parallel between our present investigation of the effect of spatial heterogeneity in vaccination coeverage, and our previous analysis of the effect of temporal heterogeneity through periodic vaccination coverage (Walter and Lion, 2021). In this previous study, the pathogen sequentially experiences two very different habitats (corresponding to maximal or minimal coverage respectively, which corresponds to $\delta = 1$ in our spatial model, and the period of fluctuations allows for varying the amount of time spent in each habitat (much like the migration parameter m). Both studies predict that heterogeneity in vaccination coverage (whether it is spatial or temporal) has no effect on the ES virulence for anti-infection and anti-transmission vaccines. However, for anti-growth and

anti-virulence vaccines, the parallel between temporal and spatial heterogeneity is not straightforward. First, the model with periodic fluctuations in vaccination coverage never predicts strain coexistence. Second, for anti-virulence vaccine, increasing the period of temporal fluctuations leads to lower virulence, whereas decreasing migration leads to higher virulence in the spatial model. Hence, the effect of increased heterogeneity is markedly different in the spatial and temporal models. This calls for further exploration of the consequences of a combination of both spatial and temporal variations in vaccine coverage on the evolution of pathogen traits. For instance, in the context of the COVID-19 pandemic, Kortessis et al. (2020) have used a similar metapopulation models to study the effect of asynchronous public health measures on disease prevalence. A very interesting avenue for future research would be to extend this analysis to explore how spatio-temporal fluctuations of the environment affect the short- and long-term evolution of pathogens. Understanding both the epidemiological and the evolutionary consequences of different deployment strategies of vaccination may help identify more effective vaccination strategy that minimze both the cumulated number cases and the speed at which the pathogen adapts to vaccination.

Funding

This work was funded by grants ANR-16-CE35-0012 "STEEP" to SL and ANR-17-CE35-0012 "EVO-MALWILD" to SG from the Agence Nationale de la Recherche.

References

Alizon, S., A. Hurford, N. Mideo, and M. Van Baalen. 2009. Virulence evolution and the trade-off hypothesis: history, current state of affairs and the future. Journal of evolutionary biology 22:245–259.

Boots, M., and A. Sasaki. 1999. 'small worlds' and the evolution of virulence: infection occurs locally and at a distance. Proceedings of the Royal Society of London B: Biological Sciences 266:1933–1938.

Day, T. 2000. Competition and the effect of spatial resource heterogeneity on evolutionary diversification. The American Naturalist 155:790–803.

Day, T., S. Gandon, S. Lion, and S. P. Otto. 2020. On the evolutionary epidemiology of sars-cov-2. Current Biology 30:R849–R857.

Day, T., D. A. Kennedy, A. F. Read, and S. Gandon. 2022. Pathogen evolution during vaccination campaigns. PLoS Biology 20:e3001804.

Débarre, F., O. Ronce, and S. Gandon. 2013. Quantifying the effects of migration and mutation on adaptation and demography in spatially heterogeneous environments. Journal of Evolutionary Biology 26:1185–1202.

Dieckmann, U., J. A. Metz, and M. W. Sabelis. 2005. Adaptive dynamics of infectious diseases: in pursuit of virulence management. 2. Cambridge University Press.

Gandon, S. 2004. Evolution of multihost parasites. Evolution 58:455–469.

Gandon, S., and T. Day. 2008. Evidences of parasite evolution after vaccination. Vaccine 26:C4–C7.

Gandon, S., T. Day, and A. Lambert. 2022. The speed of vaccination rollout and the risk of pathogen adaptation. medRxiv .

Gandon, S., and S. Lion. 2022. Targeted vaccination and the speed of sars-cov-2 adaptation. Proceedings of the National Academy of Sciences 119:e2110666119.

Gandon, S., M. Mackinnon, S. Nee, and A. Read. 2003. Imperfect vaccination: some epidemiological and evolutionary consequences. Proceedings of the Royal Society of London B: Biological Sciences 270:1129–1136.

Gandon, S., M. J. Mackinnon, S. Nee, and A. F. Read. 2001. Imperfect vaccines and the evolution of pathogen virulence. Nature 414:751.

Geritz, S. A., G. Mesze, J. A. Metz, et al. 1998. Evolutionarily singular strategies and the adaptive growth and branching of the evolutionary tree. Evolutionary ecology 12:35–57.

Gerrish, P. J., F. Saldana, B. Galeota-Sprung, A. Colato, E. E. Rodriguez, and J. X. V. Hernández. 2021. How unequal vaccine distribution promotes the evolution of vaccine escape. medRxiv .

Haraguchi, Y., and A. Sasaki. 2000. The evolution of parasite virulence and transmission rate in a spatially structured population. Journal of Theoretical Biology 203:85–96.

Hurford, A., D. Cownden, and T. Day. 2009. Next-generation tools for evolutionary invasion analyses. Journal of the Royal Society Interface 7:561–571.

Knol, M. J., A. T. Urbanus, E. M. Swart, L. Mollema, W. L. Ruijs, R. S. van Binnendijk, M. J. te Wierik, H. E. de Melker, A. Timen, and S. J. Hahné. 2013. Large ongoing measles outbreak in a religious community in the netherlands since may 2013. Euro Surveill. 18:20580.

Kortessis, N., M. W. Simon, M. Barfield, G. E. Glass, B. H. Singer, and R. D. Holt. 2020. The interplay of movement and spatiotemporal variation in transmission degrades pandemic control. Proceedings of the National Academy of Sciences 117:30104–30106.

Koutsky, L. A., and D. M. Harper. 2006. Current findings from prophylactic hpv vaccine trials. Vaccine 24:S114–S121.

Lion, S. 2018. Class structure, demography, and selection: reproductive-value weighting in nonequilibrium, polymorphic populations. The American Naturalist 191:620–637.

Lion, S., and M. v. Baalen. 2008. Self-structuring in spatial evolutionary ecology. Ecology letters 11:277–295.

Lion, S., and S. Gandon. 2021. Life-history evolution of class-structured populations in fluctuating environments. bioRxiv .

Masomian, M., Z. Ahmad, L. Ti Gew, and C. L. Poh. 2020. Development of next generation streptococcus pneumoniae vaccines conferring broad protection. Vaccines 8:132.

Mathieu, E., H. Ritchie, E. Ortiz-Ospina, M. Roser, J. Hasell, C. Appel, C. Giattino, and L. Rodés-Guirao. 2021. A global database of covid-19 vaccinations. Nature human behaviour pages 1–7.

Memish, Z. A., A. Assiri, A. Turkestani, S. Yezli, M. al Masri, R. Charrel, T. Drali, J. Gaudart, S. Edouard, P. Parola, et al. 2015. Mass gathering and globalization of respiratory pathogens during the 2013 hajj. Clinical Microbiology and Infection 21:571–e1.

Meszéna, G., I. Czibula, and S. Geritz. 1997. Adaptive dynamics in a 2-patch environment: a toy model for allopatric and parapatric speciation. Journal of Biological Systems 5:265–284.

Mirrahimi, S., and S. Gandon. 2020. Evolution of specialization in heterogeneous environments: equilibrium between selection, mutation and migration. Genetics 214:479–491.

Musher, D. M., R. Anderson, and C. Feldman. 2022. The remarkable history of pneumococcal vaccination: an ongoing challenge. Pneumonia 14:1–15.

Otto, S. P., and T. Day. 2011. A biologist's guide to mathematical modeling in ecology and evolution. Princeton University Press.

Park, A. W., J. Haven, R. Kaplan, and S. Gandon. 2015. Refugia and the evolutionary epidemiology of drug resistance. Biology letters 11:20150783.

Read, A. F., S. J. Baigent, C. Powers, L. B. Kgosana, L. Blackwell, L. P. Smith, D. A. Kennedy, S. W. Walkden-Brown, and V. K. Nair. 2015. Imperfect vaccination can enhance the transmission of highly virulent pathogens. PLoS Biology 13:e1002198.

Restif, O., and B. T. Grenfell. 2006. Integrating life history and cross-immunity into the evolutionary dynamics of pathogens. Proceedings of the Royal Society B: Biological Sciences 273:409–416.

———. 2007. Vaccination and the dynamics of immune evasion. Journal of the Royal Society Interface 4:143–153.

Ronce, O., and M. Kirkpatrick. 2001. When sources become sinks: migrational meltdown in heterogeneous habitats. Evolution 55:1520–1531.

Rousset, F. 1999. Reproductive value vs sources and sinks. Oikos 86:591–596.

Rydland, H. T., J. Friedman, S. Stringhini, B. G. Link, and T. A. Eikemo. 2022. The radically unequal distribution of covid-19 vaccinations: a predictable yet avoidable symptom of the fundamental causes of inequality. Humanities and Social Sciences Communications 9:1–6.

Schiller, J. T., and D. R. Lowy. 2012. Understanding and learning from the success of prophylactic human papillomavirus vaccines. Nature Reviews Microbiology 10:681–692.

Van Baalen, M. 2002. Contact networks and the evolution of virulence. Adaptive dynamics of infectious diseases: in pursuit of virulence management. Cambridge Univ. Press, Cambridge, UK pages 85–103.

Walter, A., and S. Lion. 2021. Epidemiological and evolutionary consequences of periodicity in treatment coverage. Proceedings of the Royal Society B 288:20203007.

Zurita-Gutiérrez, Y. H., and S. Lion. 2015. Spatial structure, host heterogeneity and parasite virulence: implications for vaccine-driven evolution. Ecology letters 18:779–789.